UDC 533.3+611.539

MODELLING OF THE ACOUSTIC PROPERTIES OF THE LARGER HUMAN BLOOD VESSEL

A. O. BORISYUK

Institute of Technical Acoustics, Department of Electrical Engineering, Dresden University of Technology, Dresden, Germany, (permanent affiliation: Institute of Hydromechanics of NAS of Ukraine, Kyiv)

Received 27.08.98

An acoustic model of a larger human blood vessel is developed in order to study the properties of an acoustic field produced by a stenotic narrowing in vessel. This model accounts of the basic features of the generation and propagation of noise in the human chest from the source (turbulent pressure fluctuations in blood flow) to a receiver resting on the skin. The low Mach number turbulent wall pressure models of Corcos, Chase, Ffowcs Williams and Smol'yakov – Tkachenko are used to describe random noise sources in the vessel. The relationships obtained permit one to analyse the dependence of the acoustic field in the thorax on the parameters of the blood flow and the vessel, and give the possibility of finding characteristic signs of the presence of a stenotic narrowing in vessel.

INTRODUCTION

The diagnosis of stenotic obstructions of vessels is of a great concern to the medical clinician. The most common method for obtaining information on a stenosis is through the use of arteriograms. This is, however, an *invasive* technique which is often expensive, uncomfortable for the patient, involves risk of infection and bleeding, and it is usually only used when the disease is rather advanced and accompanied by other symptoms. Of particular value therefore are alternative diagnostic procedures which are *non-invasive*. Since a stenosis creates a number of abnormal flow conditions in the vessel, several non-invasive techniques based on these abnormalities have been suggested in the last few decades [1 – 8].

One such technique is called the method of *phonoangiography*. It was initially proposed by Lees and Dewey [8] and has subsequently been studied and applied extensively by many researchers [9 – 20]. This method uses the pressure field induced in vessels and perceived at the skin surface as sound. The mean statistical characteristics of the sound field can then be found and analysed in order to obtain the information about stenosis (such as the presence, location, shape, characteristic dimensions, etc.). However, quantitative diagnosis of a stenosis is only possible if the fundamental mechanisms of vascular sound generation and transmission are known. There is a number of studies [8 – 12, 19 – 22], which suggest that the most probable sources of blood motion sound are turbulent pressure fluctuations in the flow.

At present several low Mach number models of the pressure fluctuations are available. They can be used in constructing an acoustic model of a lager human blood vessel. Such a model must correctly describe the rheological properties of blood and the nature of the flow in the vessel, the physical and geometrical characteristics of the vessel, the stenotic obstruction, the structure and acoustical properties of the human body tissue, etc. As a result, it will correctly describe the generation and transmission of noise from the source to the receiver resting on the skin which is necessary for solving the *inverse* problem (viz. locating pathology by changes in the characteristics of noise field picked up from the chest surface of a given patient).

Analysis of the scientific literature shows that the creation of an acoustic model of a separate vessel is still far from complete. To the author's knowledge, at present only a few works [17, 22 – 25] can be reported in which the simplest models are introduced. Some of them are the models of a larger airway of the human respiratory system [17, 23 – 25] (nevertheless, these models can be easily adapted to the case of a larger blood vessel for the corresponding parameter values). Although undoubtadly important, these works have, however, some disadvantages. Namely, in the model suggested by Wodicka et al. [23, 24] the source of sound is represented by a determined loading at the inner surface of an infinite circular pipe, and the body is introduced as an infinite homogeneous medium of known density, sound speed and damping coefficient. Such an approach does not take into account neither the finiteness of the human body volume nor the random statistical nature of loading.

A few years later Vovk et al. [17] have outlined a simple qualitative model which looked much similar to that developed by Wodicka et al. [23, 24].

In the more recent paper by Vovk et al. [25] two finite coaxial circular cylinders with random turbulent pressures at the surface of the inner cylinder were considered. This is more realistic approach com-

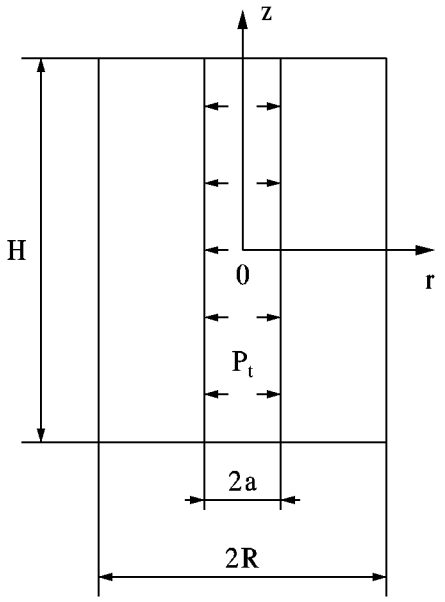

Fig. 1. Acoustic model of a larger human blood vessel

pared with the previous ones. However, here the authors have not considered the presence of a stenotic constriction in the vessel. In addition, they have used the Corcos model [26] for turbulent wall pressure fluctuations, the disadvantages of which are well known [27,28].

Wong et al. [22] have been likely the first who made the attempt to describe a vascular stenosis. Their model consisted of two finite, joined in series, isolated elastic cylinders excited by inner random turbulent forces. One cylinder simulated an arterial stenosis, and the other was a poststenotic segment of an artery. In general, such approach looks interesting. However, to be used in practice, it requires some clarifications and completions to be made. Namely, the boundary conditions for the cylinders and the turbulent wall pressure field, as well as the influence of the body tissue on a sound field have to be discribed more adequately.

This paper presents an acoustic model of a larger human blood vessel. This model takes account of all the above mentioned basic features of the generation and transmission of noise in the human chest from the source to the receiver, and permits consideration of a stenotic narrowing in the vessel. The formulation of the model and the corresponding assumptions with respect to the ranges of its applicability are given in Section 2. Section 3 briefly describes the incompressible turbulent wall pressure models which are used in the study. The analytical solution for the noise field in the thorax is constructed and qualitatively analysed in Section 4. The numerical analysis of the noise field and its dependence on the parameters of the vessel and the blood flow is carried out in Section 5. Finally, the conclusions of the investigation are summarized in Section 6.

1. ACOUSTIC MODEL

The nature and character of the blood loading in vessels, as well as the geometry and the physical properties of the blood vessels and surrounding body tissue are extremely complicated. This is the reason for the absence of satisfactory information about them. Under these circumstances precise modelling of the vascular sound generation and transmission is extremely difficult, and at present the question can be only about making approximate gradual steps to constructing an acoustic model of a larger blod vessel. They must be based on the generally accepted assumptions and available data [1, 2, 17, 22–25].

Taking this into account we restrict ourselves to consideration of the axisymmetric, quasy-steady, fully developed turbulent flow in the vessel, two-phase acoustic medium as the body tissue and the cylindrical shape for the human chest. These allow us to formulate the acoustic model of a larger blood vessel. The geometry of the model is shown in fig. 1. Here the human thorax is represented by a finite circular cylinder, of height H and radius R, filled with an acoustic medium of density ρ_0 and sound speed c_0 and surrounded by air. The vessel is simulated by a finite coaxial circular pipe, of the same height H and radius a ($a \ll R$). The turbulent blood flow in the pipe is characterised by mean velocity U determinable as the ratio of the flow rate, averaged over a cardiac cycle, to the cross-sectional area of the vessel. Blood has density ρ and sound speed c. Turbulent pressure fluctuations at the inner surface of the vessel ($r=a$) radiate sound waves that can be detected at the body surface ($r=R$) by a special detector. The mean statistical characteristics of these sounds can then be determined and analysed in order to diagnose the vessel condition.

The corresponding axisymmetric mathematical problem is governed by the two-dimensional wave equation in the radial, r, and axial, z, coordinates

$$\nabla^2_{(r,z)} p_0 - \frac{1}{c_0^2}\frac{\partial^2 p_0}{\partial t^2} = 0 \qquad (1)$$

and the following boundary conditions

$$p_0|_{r=a} = p_t, \quad p_0|_{r=R} = 0, \quad p_0|_{z=\pm H/2} = 0. \qquad (2)$$

Here $p_0(r,z,t)$ and $p_t(z,t)$ are the acoustic and bulent pressures, respectively, and the origin of cylindrical coordinate system is taken in the ce of the cylinders. The random turbulent pressure $p_t(z,t)$ is assumed to be temporally stationary spatially homogeneous.

The last two conditions in (2) are due to the wave resistance of the body tissue is n higher than that of air (i.e., $\rho_0 c_0 \approx 9000$ kg/ $(\rho c)_{air} \approx 420$ kg/m^{2}s).

In generating noise by constricted vessel, many tors play significant role [29, 30]. These are the st sis geometry and the vessel geometry, velocity and waveform of the flow, viscosity and density of the fluid, etc. The most important of these are the ratio of the minimum cross sectional area, A, to the unobstructed lumen area, A_0, of the vessel (or the stenosis severity, $(1-A/A_0)\times 100\%$) and the mean flow velocity. The above formulated model permits consideration of a simple stenotic narrowing which is characterized by the ratio A/A_0, viz.

$$\begin{aligned} \text{intact vessel} \quad &: \quad a = a_0, \\ \text{narrowed vessel} \quad &: \quad a = \gamma a_0, \end{aligned} \tag{3}$$

($\gamma^2 = A/A_0$, $0<\gamma<1$), and, via the mass conservation condition in the narrowed and intact arteries, viz.

$$uA = UA_0, \tag{4}$$

takes into account the corresponding changes in the mean flow velocity in the constriction, viz.

$$u = U(A_0/A) = U/\gamma^2. \tag{5}$$

The arterial narrowing (3) causes not only the increase in the blood flow energy (i.e. from $E_0 \sim U^2$ in the normal artery to $E \sim u^2$ in the diseased artery) but also redistribution of the turbulence energy on the flow scales (i.e. from eddies of dimensions of order $D/2$ convecting at speeds U and U_c in the intact pipe to eddies of dimensions of order $d/2$ convecting at speeds $u=U/\gamma^2$ and $u_c=U_c/\gamma^2$ in the obstructed pipe). These changes in the sound source structure will cause both the increase in the radiated acoustic power levels and the appearance of the new frequency components in the sound field characteristics which are reported in periodicals. Consequently, these sound field variations can be used as the indicators of changes in the vessel state.

2. TURBULENT WALL PRESSURE MODELS

Much work has been made in the past to describe pressure fluctuations beneath an incompressible turbulent boundary layer [27, 31]. However, at the present time only several empirical and semiempirical models for the wavenumber-frequency spectrum of turbulent wall pressure are available [26, 32–34] which are more or less acceptable for practice [27]. The first of these was proposed by Corcos [26]. Following his ideas, the cross-spectrum $S_p(\xi,\omega)$ of a statistically stationary and homogeneous one-dimensional wall pressure field, $p_t(z,t)$, at two arbitrary space-time points (z,t) and $(z+\xi, t+\tau)$ can be written as

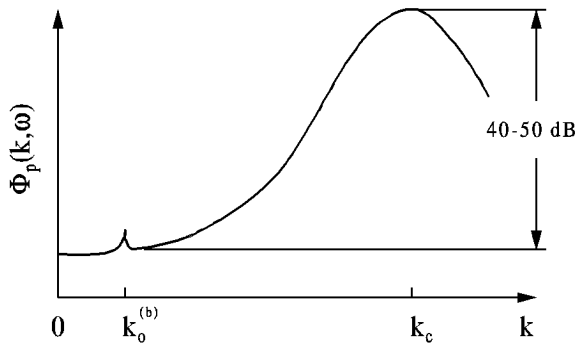

Fig. 2. Wavenumber-frequency spectrum $\Phi_p(k,\omega)$ of turbulent wall pressure with $\omega=$const

$$S_p(\xi,\omega) = P(\omega)\,A(\omega\xi/U_c)e^{-i\omega\xi/U_c}, \tag{6}$$

where $P(\omega)$ and $A(\omega\xi/U_c)$ are the power (or frequency) spectrum and normalized to unity cross-spectrum (i.e. $A(0)=1$) of pressure fluctuations, respectively. In practice [26,27,31], $A(\omega\xi/U_c)$ is frequently approximated by exponential decay function,

$$S_p(\xi,\omega) = P(\omega)e^{-\beta|\omega\xi/U_c|}e^{-i\omega\xi/U_c}, \tag{7}$$

in which β is a parameter chosen to yield the best agreement with experiment. Substituting formula (7) into expression relating cross-spectrum, $S_p(\xi,\omega)$, to wavenumber-frequency spectrum, $\Phi_p(k,\omega)$, i.e.

$$\Phi_p(k,\omega) = (1/2\pi)\int_{-\infty}^{\infty} S_p(\xi,\omega)e^{-ik\xi}d\xi, \tag{8}$$

yields the Corcos model for $\Phi_p(k,\omega)$:

$$\Phi_p(k,\omega) = P(\omega)\frac{\beta}{\pi[(kU_c/\omega-1)^2+\beta^2]}. \tag{9}$$

Function (9) describes quite well the structure of the wavenumber-frequency spectrum of the wall pressure only in the range of the convective wavenumber, $k \approx k_c = \omega/U_c$, where $\Phi_p(k,\omega)$ is sharply peaked, owing to the convective nature of the turbulence (see fig. 2). Consequently, when the total noise field

generated by turbulence is dominated by the convective wall pressure components, then the Corcos model gives satisfactory predictions of noise. However, when the subconvective wall pressure components, $k \ll k_c$, dominate, then the Corcos model highly overpredicts the actually generated noise levels. This is because the spectral levels at wavenumbers below the convective peak in spectrum (9) are $25-35$ dB higher than the available experimental data [27, 28, 31]. The other disadvantage of expression (9) is that it violates the k^2 dependence of the low-wavenumber spectrum as k approaches zero [27].

More recent models by Chase [32], Ffowcs Williams [33] and Smol'yakov–Tkachenko [34] have been designed to describe the subconvective region more accurately. The various approaches have been used herewith. In contrast to the purely empirical Corcos model, which has been constructed proceed from examination of published experimental data, the semiempirical Chase model [32] was based on consideration of contributions of mean shear and pure turbulence to the spectrum of the wall pressure. His model, adapted to the case of one-dimensional flow, is

$$\Phi_p(k,\omega) = \rho^2 v_*^3 [c_M k^2 K_M^{-5} + c_T k^2 K_T^{-5}],$$
$$K_i^2 = (\omega - U_c k)^2/(h_i v_*)^2 + k^2 + (b_i\delta)^{-2}, \qquad (10)$$
$$i = M, T,$$

With the dimensionless coefficients $h_M \approx h_T \approx 3$, $c_T = 0.0474$, $c_M = 0.0745$, $b_T = 0.378$ and $b_M = 0.756$, recommended by Chase, expression (10) can predict a convective pressure level which agrees well with the experimentally measured, and it displays the k^2 dependence in the low-wavenumber domain.

Ffowcs Williams [33] started from Lighthill's acoustic analogy and assumed that the velocity source terms were of the general Corcos form. His final expression for the wavenumber-frequency spectrum has the k^2 dependence in the low-wavenumber range and accounts of the effects of compressibility. However, it contains a number of unknown constants and functions to be determined experimentally. To date, these remain unknown, but Hwang & Geib [35] have proposed a simplified version, which neglects the effects of compressibility and assumes a specific form for the remaining functions. The one-dimensional version of their expression, slightly adjusted to agree with the Corcos parameters, is

$$\Phi_p(k,\omega) = P(\omega)[kU_c/\omega]^2 \frac{\beta}{\pi[(kU_c/\omega - 1)^2 + \beta^2]}, \quad (11)$$

Smol'yakov and Tkachenko [34] fitted exponential curves to their measured cross-spectral densities. However, in contrast to Corcos, who directly multiplied his pure longitudinal and pure lateral cross-spectra, they took the compbined cross-spectrum to be of more sophisticated form, and Fourier transformed their expression. The one-dimensional version of their wavenumber-frequency spectrum is

$$\begin{aligned}
\Phi_p(k,\omega) &= 0.025 P(\omega) A(\omega) h(\omega) (U_c/\omega)^2 \times \\
&\times [F(k,\omega) - \Delta F(k,\omega)], \\
A(\omega) &= 0.124[1 - 0.2/\omega^* + (0.2/\omega^*)^2]^{1/2}, \\
\omega^* &= \omega\delta^*/U, \\
F(k,\omega) &= [A^2 + (1 - U_c k/\omega)^2]^{-3/2}, \\
\Delta F(k,\omega) &= 0.995\Big[A^2 + 1 + (1.005/m_1)\times \\
&\times [(m_1 - U_c k/\omega)^2 - m_1^2]\Big]^{-3/2}, \\
m_1 &= (A^2+1)/(1.025 + A^2), \\
h(\omega) &= [1 - 0.153A(A^2+1)/((1.025 + A^2)\times \\
&\times (0.02 + A^2))^{1/2}]^{-1},
\end{aligned} \qquad (12)$$

Although Smol'yakov and Tkachenko gave arguments and reported experimental results supporting their model, expression (12) violates the k^2 behaviour of the spectrum $\Phi_p(k,\omega)$ at low wavenumbers.

3. ANALYSIS OF THE SOUND FIELD IN THE THORAX

The solution to the formulated boundary problem (1), (2) is obtained by taking the Fourier transform, defined here with the convention

$$g(k,\omega) = \frac{1}{(2\pi)^2} \int_{-H/2}^{H/2} \int_{-\infty}^{\infty} g(z,t) e^{-i(kz - \omega t)} dz dt, \quad (13)$$

and expanding the acoustic pressure $p_0(r,z,\omega)$ into an infinite series of trigonometric functions and cylindrical Bessel functions of zero order, viz.

$$\begin{aligned}
p_0(r,z,\omega) = \sum_{n=1}^{\infty} \Big(&\cos(\beta_n^{(1)} z)\times \\
&\times \big[A_n^{(1)} J_0(\alpha_n^{(1)} r) + B_n^{(1)} Y_0(\alpha_n^{(1)} r)\big] + \\
&+ \sin(\beta_n^{(2)} z)\times \\
&\times \big[A_n^{(2)} J_0(\alpha_n^{(2)} r) + B_n^{(2)} Y_0(\alpha_n^{(2)} r)\big]\Big),
\end{aligned} \qquad (14)$$

where the axial wavenumbers $\beta_n^{(1)}$, $\beta_n^{(2)}$ and radial wavenumbers $\alpha_n^{(1)}$, $\alpha_n^{(2)}$ are given by the following expressions

$$\begin{aligned} \beta_n^{(1)} &= (2n-1)\pi/H, \quad & \alpha_n^{(1)} &= \sqrt{k_0^2-(\beta_n^{(1)})^2}, \\ \beta_n^{(2)} &= 2n\pi/H, & \alpha_n^{(2)} &= \sqrt{k_0^2-(\beta_n^{(2)})^2}. \end{aligned} \tag{15}$$

In relationship (14), the acoustic modes $\Psi_n^{(1)}(z)=\cos(\beta_n^{(1)}z)$ and $\Psi_n^{(2)}(z)=\sin(\beta_n^{(2)}z)$ of the chest volume describe the symmetric and antisymmetric parts of the random sound field $p_0(r,z,\omega)$, respectively (with respect to the plane $z=0$), and the Bessel functions $J_0(\ldots)$ and $Y_0(\ldots)$ describe the radial distribution of the field.

In the form taken, solution (14) satisfies the two-dimensional Helmholtz equation

$$\nabla^2_{(r,z)}p_0(r,z,\omega)+k_0^2p_0(r,z,\omega)=0, \tag{16}$$

with acoustic wavenumber $k_0=\omega/c_0$ in the body tissue, and the boundary conditions (2) on the upper side, $z=H/2$, and lower side, $z=-H/2$, of the outer cylinder. The unknown amplitudes $A_n^{(j)}$ and $B_n^{(j)}$ can be obtained from the conditions (2) at the surfaces of the inner and outer pipes by the use of the orthogonality properties of the acoustic modes $\Psi_n^{(j)}(z)$ $(j=1,2)$, viz.

$$\int_{-H/2}^{H/2}\Psi_n^{(1)}(z)\Psi_m^{(2)}(z)dz=\begin{cases} 0, & \text{for } m=n \\ 0, & \text{for } m\neq n, \end{cases}$$

$$\int_{-H/2}^{H/2}\Psi_n^{(j)}(z)\Psi_m^{(j)}(z)dz=\begin{cases} H/2, & \text{for } m=n \\ 0, & \text{for } m\neq n. \end{cases}$$

After finding the coefficients $A_n^{(j)}$ and $B_n^{(j)}$, the final expression for the random acoustic pressure $p_0(r,z,\omega)$ takes the form

$$\begin{aligned} p_0(r,z,\omega) &= \sum_{n=1}^{\infty}\big[\cos(\beta_n^{(1)}z)\times \\ &\times\big(G(\alpha_n^{(1)},r,R)/G(\alpha_n^{(1)},r=a,R)\big)p_{t_n}^{(1)}(\omega)+ \\ &+\sin(\beta_n^{(2)}z)\times \\ &\times\big(G(\alpha_n^{(2)},r,R)/G(\alpha_n^{(2)},r=a,R)\big)p_{t_n}^{(2)}(\omega)\big]. \end{aligned} \tag{17}$$

Here the term that defines the degree of excitation of the acoustic mode $\Psi_n^{(j)}(z)$ by the random turbulent pressure p_t is given by the expression

$$p_{t_n}^{(j)}(\omega)=\frac{2}{H}\int_{-H/2}^{H/2}p_t(\eta,\omega)\Psi_n^{(j)}(\eta)d\eta, \quad (j=1,2),$$

and

$$\begin{aligned} G(\alpha_n^{(j)},r,R) &= Y_0(\alpha_n^{(j)}R)J_0(\alpha_n^{(j)}r)- \\ &-J_0(\alpha_n^{(j)}R)Y_0(\alpha_n^{(j)}r) \end{aligned}$$

is a combination of the Bessel functions.

Since in the framework of the model under consideration the acoustic pressure vanishes at the chest surface, the basic parameter of the noise field recorded from patients is the radial acceleration [17,25], viz.

$$\begin{aligned} w_r(r,z,\omega) &= -(1/\rho_0)\partial p_0(r,z,\omega)/\partial r = \\ &= (1/\rho_0)\sum_{n=1}^{\infty}[\cos(\beta_n^{(1)}z)\alpha_n^{(1)}\times \\ &\times(F(\alpha_n^{(1)},r,R)/G(\alpha_n^{(1)},r=a,R))p_{t_n}^{(1)}(\omega)+ \\ &+\sin(\beta_n^{(2)}z)\alpha_n^{(2)}\times \\ &\times(F(\alpha_n^{(2)},r,R)/G(\alpha_n^{(2)},r=a,R))p_{t_n}^{(2)}(\omega)], \end{aligned} \tag{18}$$

where the function $F(\alpha_n^{(j)},r,R)$ is, like $G(\alpha_n^{(j)},r,R)$, written in terms of cylindrical Bessel functions, viz.

$$\begin{aligned} F(\alpha_n^{(j)},r,R) &= Y_0(\alpha_n^{(j)}R)J_1(\alpha_n^{(j)}r)- \\ &-J_0(\alpha_n^{(j)}R)Y_1(\alpha_n^{(j)}r), \quad j=1,2. \end{aligned}$$

The spectral density $P_w(r,z,\omega)$ of the random field $w_r(r,z,\omega)$ at the measurement point (r,z) can be obtained from the relationship of statistical orthogonality [31], i. e.

$$P_w(r,z,\omega)\delta(\omega-\omega')=\langle w_r^*(r,z,\omega)\ w_r(r,z,\omega')\rangle, \tag{19}$$

in which the brackets denote an ensemble average, $\delta(\ldots)$ is the Dirac delta function, and the asterisk denotes a complex conjugate. When the radial acceleration (18) is substituted into expression (19), and the required operations are performed, the spectral

density becomes

$$P_w(r,z,\omega) = \sum_{n=1}^{\infty}(P_w(r,z,\omega))_n =$$
$$= (2/\rho_0 H)^2 \sum_{n=1}^{\infty}[\cos^2(\beta_n^{(1)}z)|\alpha_n^{(1)}|^2 \times$$
$$\times(|F(\alpha_n^{(1)},r,R)|^2/|G(\alpha_n^{(1)},r=a,R)|^2)\Phi_{p_n}^{(1)}(\omega)+ \quad (20)$$
$$+\sin^2(\beta_n^{(2)}z)|\alpha_n^{(2)}|^2 \times$$
$$\times(|F(\alpha_n^{(2)},r,R)|^2/|G(\alpha_n^{(2)},r=a,R)|^2)\Phi_{p_n}^{(2)}(\omega)],$$

where $\Phi_{p_n}^{(j)}(\omega)$ $(j=1,2)$ are the modal excitation terms, defined in terms of the wavenumber-frequency spectrum of the turbulent wall pressure, $\Phi_p(k,\omega)$, and the shape functions of the thorax volume

$$|S_n^{(1)}(k)|^2 = 4(\beta_n^{(1)})^2\cos^2(kH/2)/[k^2-(\beta_n^{(1)})^2]^2,$$

$$|S_n^{(2)}(k)|^2 = 4(\beta_n^{(2)})^2\sin^2(kH/2)/[k^2-(\beta_n^{(2)})^2]^2$$

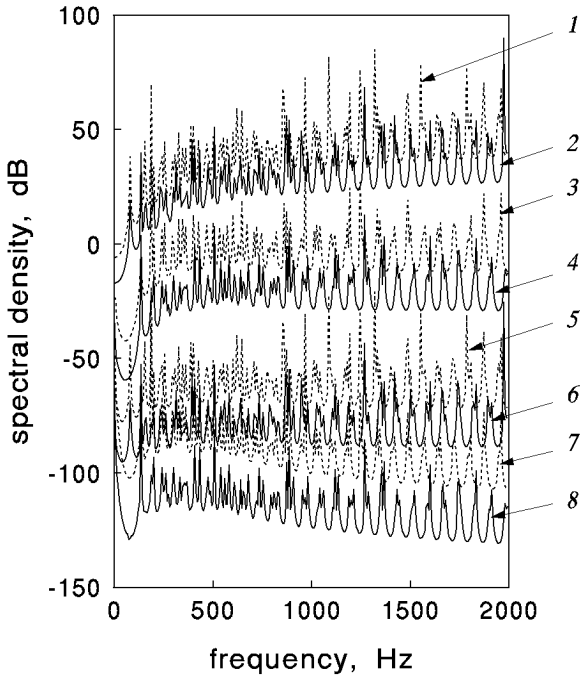

Fig. 3. Spectra of the thorax surface radial acceleration at point $(r=R,\ z=0)$ produced by turbulence in a normal (solid lines, $\mathrm{Re}_{a_0}=3500$) and narrowed (dashed lines, $\gamma=0.7$; $S=(1-\gamma^2)\times 100\%=51\%$; $\mathrm{Re}_{\gamma a_0}=5000$) vessels at the flow velocity $U=0.7$ m/s, as calculated for the Corcos (curves *1* and *2*), Ffowcs Williams (curves *3* and *4*), Smol'yakov-Tkachenko (curves *5* and *6*), and Chase (curves *7* and *8*) models

as

$$\Phi_{p_n}^{(j)}(\omega) = \int_{-\infty}^{\infty}|S_n^{(j)}(k)|^2\Phi_p(k,\omega)dk. \quad (21)$$

Thus, the spectral density, $P_w(r,z,\omega)$, of a radial acceleration at the measurement point (r,z) is a sum of individual mode contributions, $(P_w(r,z,\omega))_n$. The modal spectral densities are determined by the two factors. Firstly, this is the degree of excitation of the acoustic mode, $\Psi_n^{(j)}(z)$, which is represented by the modal excitation term $\Phi_{p_n}^{(j)}(\omega)$. This term depends on the amplitudes of the wall pressure components and their spatial correlations with the mode $\Psi_n^{(j)}(z)$. Secondly, this is the term $|\Psi_n^{(j)}(z)|^2\cdot|\alpha_n^{(j)}|^2\cdot|F(\alpha_n^{(j)},r,R)|^2/|G(\alpha_n^{(j)},r=a,R)|^2$ which is in fact the transfer function of the thorax. It contains the geometrical characteristics of the vessel and thorax, and the acoustical properties of the body volume (such as cut-off frequencies, acoustic resonances), and describes propagation of the sound waves from the source to the receiver.

All information with respect to the flow in the vessel is contained in the wavenumber-frequency spectrum, $\Phi_p(k,\omega)$, of the turbulent wall pressure, and hence, via formulas (20) and (21), in the spectrum $P_w(r,z,\omega)$. Any changes in the flow structure will result in the changes in the turbulent source structure (i.e. increase of the turbulence energy and its redistribution on the flow scales), which are then reflected in the function $P_w(r,z,\omega)$. Therefore, this mean statistical characteristic of the random signal recorded from the chest surface can be used to diagnose the vessel condition by changes in the structure of the noise field produced by the flow. This property of the radial acceleration power spectrum is actually used by physician in diagnosing patients.

4. NUMERICAL ANALYSIS AND DISCUSSION

In calculating the spectral density (20), the following values of the geometrical and physical parameters of the model have been used: $a_0=1$ cm, $R=0.2$ m, $H=0.4$ m, $\rho=1050$ kg/m^3, $c=1500$ m/s, $\nu=4\times10^{-6}$ m^2/s, $\rho_0=300$ kg/m^3, $c_0=30$ m/s, $U=0.4\div1$ m/s, $f=\omega/2\pi=1$ Hz $\div$ 2 kHz. These magnitudes agree well with those cited in periodicals [23–25, 29, 30, 36], and are typical for patients.

The predictions for the noise spectra $10\lg[P_w(r,z,f)/(P_w(f))_0]$ (where $(P_w(f))_0 = (2/\rho_0 H)^2 P(f)$; $P_w(f)=4\pi P_w(\omega)$ [31]), obtained for the turbulent pressure fluctuations models (9)–(12), are shown in fig. 3. Here the sol-

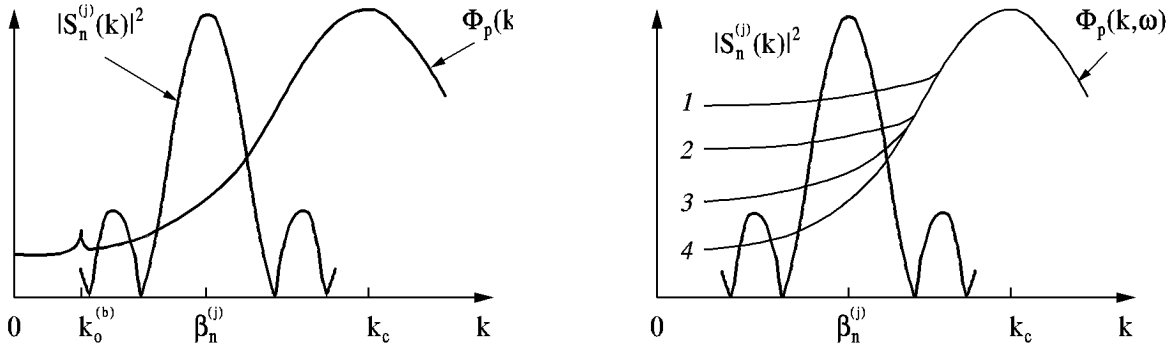

Fig. 4. Behaviour of the shape function $|S_n^{(j)}(k)|^2$ and wavenumber-frequency spectrum $\Phi_p(k,\omega)$ with $\omega=\text{const}$:
a – behaviour of $|S_n^{(j)}(k)|^2$ and $\Phi_p(k,\omega)$ with $\omega=\text{const}$ under the integral sign in (21);
b – approximate behaviour of different models for $\Phi_p(k,\omega)$ with $\omega=\text{const}$,
1 – the Corcos model; 2 – Ffowcs Williams model; 3 – Smol'yakov–Tkachenko model; 4 – Chase model

id lines correspond to a normal vessel ($\text{Re}_{a_0} = U(2a_0)/\nu = 3500$) and dashed lines correspond to a narrowed vessel ($\gamma=0.7$, $\text{Re}_{\gamma a_0} = u(2\gamma a_0)/\nu = \text{Re}_{a_0}/\gamma = 5000$).

One can see that the acoustic model predicts that pipe constriction may be identified by comparison of the noise fields produced by intact and obstructed vessels. Since the flow energy in a narrowed pipe ($E\sim u^2$) is higher than that in a normal pipe ($E_0\sim U^2$), the noise field generated by the more powerful turbulent sources in a partially occluded vessel is of higher intensity compared to that from the less powerful sources in a normal vessel. The difference between the spectral levels of these noise fields is significant and, as well as the noise levels themselves, depends on the turbulence model used.

The physical basis of this dependence is illustrated in fig. 4. This figure shows the wavenumber dependence of the shape function $|S_n^{(j)}(k)|^2$ and spectrum $\Phi_p(k,\omega)$ in the modal excitation term (21). In general case, the main contribution to the spectrum $\Phi_{p_n}^{(j)}(\omega)$ comes from the main lobe of the oscillating function $|S_n^{(j)}(k)|^2$ at subconvective wavenumber $k=\beta_n^{(j)} \ll k_c$ and from the convective peak of the smooth function $\Phi_p(k,\omega)$ at $k=k_c$ (see fig. 4, a), viz.

$$\Phi_{p_n}^{(j)}(\omega) \approx (\Phi_{p_n}^{(j)}(\omega))_{\text{subconv}} + (\Phi_{p_n}^{(j)}(\omega))_{\text{conv}} = \\ = \Big(\int\limits_{\text{subconv}} + \int\limits_{\text{conv}}\Big)|S_n^{(j)}(k)|^2\Phi_p(k,\omega)\,dk. \qquad (22)$$

As noted in the section 3, the turbulent wall pressure models by Corcos, Ffowcs Williams, Smol'yakov–Tkachenko, and Chase approximate the convective domain of the spectrum $\Phi_p(k,\omega)$ equally well, but they differ from each other in the subconvective range (see fig. 4, b). Consequently, when the total noise field from turbulence is dominated by the convective wall pressure components, viz.

$$(\Phi_{p_n}^{(j)}(\omega))_{\text{subconv}} \ll (\Phi_{p_n}^{(j)}(\omega))_{\text{conv}}, \qquad (23)$$

then all the turbulence models give the same predictions of noise, viz.

$$\Phi_{p_n}^{(j)}(\omega) \approx (\Phi_{p_n}^{(j)}(\omega))_{\text{conv}} = \\ = ((\Phi_{p_n}^{(j)})_{\text{conv}})_{\text{Corcos}} = ((\Phi_{p_n}^{(j)})_{\text{conv}})_{\text{F. W.}} = \\ = ((\Phi_{p_n}^{(j)})_{\text{conv}})_{\text{Sm.–Tk.}} = ((\Phi_{p_n}^{(j)})_{\text{conv}})_{\text{Chase}}.$$

However, when the contribution from the subconvective wall pressure components is either of the same order of magnitude as that from the convective components, viz.

$$(\Phi_{p_n}^{(j)}(\omega))_{\text{subconv}}/(\Phi_{p_n}^{(j)}(\omega))_{\text{conv}} = O(1), \qquad (24)$$

or dominates, viz.

$$(\Phi_{p_n}^{(j)}(\omega))_{\text{subconv}} \gg (\Phi_{p_n}^{(j)}(\omega))_{\text{conv}}, \qquad (25)$$

then, due to the different values of the first term on the right side in (22), the turbulence models (9) – (12) give different predictions of noise.

Inequality (23) takes place in case of high Mach number flows (i. e. $k_0^{(b)}/k_c = U_c/c \le 1$ or $k_0^{(b)}/k_c > 1$), whereas relationships (24) and (25) are associated with low and extremely low Mach number flows, respectively. Since blood flow in the vessel is characterized by extremely low Mach numbers

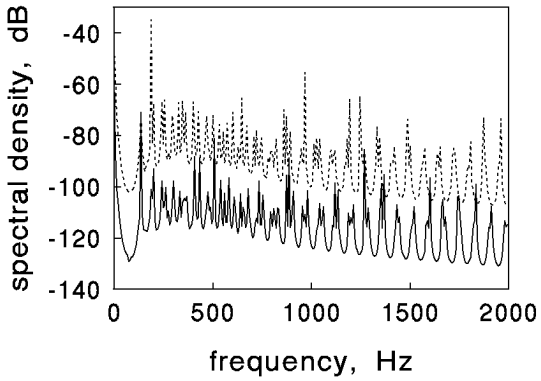

Fig. 5. Spectra of the thorax surface radial acceleration at point ($r=R$, $z=0$) produced by turbulence in a normal (solid line; $\mathrm{Re}_{a_0}=3500$) and constricted (dashed line; $\gamma=0.7$; $S=51\%$; $\mathrm{Re}_{\gamma a_0}=5000$) vessels at the flow velocity $U=0.7$ m/s, as calculated for the Chase model

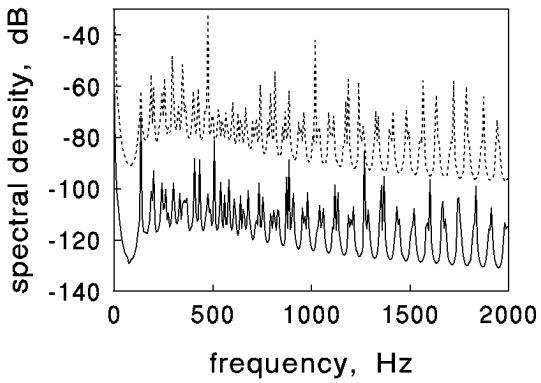

Fig. 6. Spectra of the thorax surface radial acceleration at point ($r=R$, $z=0$) produced by turbulence in a normal (solid line; $\mathrm{Re}_{a_0}=3500$) and constricted (dashed line; $\gamma=0.6$; $S=64\%$; $\mathrm{Re}_{\gamma a_0}=5833$) vessels at the flow velocity $U=0.7$ m/s, as calculated for the Chase model

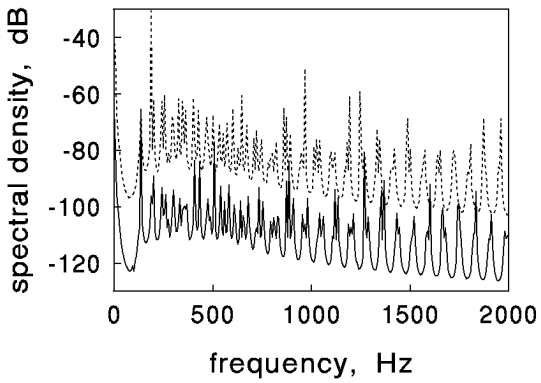

Fig. 7. Spectra of the thorax surface radial acceleration at point ($r=R$, $z=0$) produced by turbulence in a normal (solid line; $\mathrm{Re}_{a_0}=4500$) and constricted (dashed line; $\gamma=0.7$; $S=51\%$; $\mathrm{Re}_{\gamma a_0}=6429$) vessels at the flow velocity $U=0.9$ m/s, as calculated for the Chase model

($M=U/c<10^{-3}$ for the physiological range of flow velocities $U<1$ m/s), the case (25) takes place in this study. This explains the differences between the noise predictions for the various turbulence models.

The most important feature of the data shown in fig. 3 is that one cannot precisely superpose the corresponding dashed and solid lines by parallel displacement. This is due to the redistribution of the turbulence energy on the different flow scales and production of the new frequency components in the power spectrum. The redistribution of the turbulence energy on the flow scales in a narrowed pipe and the corresponding production of the new frequency components in the acceleration power spectrum (20) is associated with the displacement of the convective peak at $k_c=\omega/U_c$ in a normal vessel to $k_c^{(d)}=\gamma^2 k_c$ in a narrowed vessel.

The other feature of the curves in fig. 3 is connected with the existence of the great amount of spectral peaks. The maxima in the spectra are identified with the acoustic resonances of the chest volume. These resonances are contained in the denominators $|G(\alpha_n^{(j)}, r=a, R)|^2$ in expression (20), and their number is determined by the chosen values of the acoustic model parameters.

As noted in the introduction, the authors of the acoustic model [25] have used the Corcos cross-spectrum (7) to describe random pressures at the vessel surface. The above given comparative analysis of the noise predictions for the various turbulent wall pressure models shows that the Corcos spectrum will overestimate the sound levels in the physiological ranges of the flow parameter values. This makes investigators to be careful in applying this model to describe turbulent sources in the vessel.

The other models in the section 3 simulate the structure of the near-wall turbulence in the subconvective region better than the Corcos model. The estimates of the acoustic fields obtained for the Chase, Ffowcs Williams, and Smol'yakov–Tkachenko spectra, and their comparison with the available experimental data show that the Chase model gives the best predictions for these fields [27]. It is therefore further used in this work for the analysis of the sound field.

Having given the arguments in favour of the Chase model, let us consider fig. 5 and 6 which present the noise spectra (dashed lines) produced by constricted pipes of different diameters (fig. 5: $\gamma=0.7$, $\mathrm{Re}_{\gamma a_0}=5000$, and fig. 6: $\gamma=0.6$, $\mathrm{Re}_{\gamma a_0}=5833$) at the same flow velocity. These curves demonstrate the influence of the constriction severity

$$S=(1-A/A_0)\times 100\%=(1-\gamma^2)\times 100\%$$

on the noise field. Their comparison shows that the role of this parameter is reflected in the different degree of turbulence of a flow. The higher S (viz. the smaller γ) the higher the turbulence intensity in the narrowed pipe, and therefore the higher the generated noise intensity. This agrees well with the available experimental data [20, 29, 30] which indicate that stronger stenosis produces higher noise levels, and therefore becomes easier to be detected by a physician.

Although the influence of mean flow velocity, U, on a noise field generated is qualitatively similar to that of a constriction severity (i.e., an increase of noise levels due to an increase of a velocity), medical interpretation of this effect is different. Namely, it is well known in medical practice that a stenosis in a given patient cannot be detected under resting flow conditions (the patient rests), but it becomes detectable under elevated flow conditions (manual labour). This is because the difference between the levels of noise from diseased and normal vessels increases as the flow velocity increases. This is demonstrated in fig. 5 and 7 in which the noise spectra produced by intact vessel and the same narrowed vessel at different flow velocities are shown. The difference is seen to be rather sensitive to small changes in the mean flow velocity, U.

CONCLUSIONS

The character of blood flow in a larger vessel and the properties of blood vessel and surrounding body tissue are complicated, and the available information about them is restricted and incomplete. The appearance of a vascular stenosis causes significant changes in the flow structure, such as the appearance of a region of a fully developed turbulence, increase of the flow energy, redistribution of the energy on different flow scales, etc. These result in the increase of the acoustic power generated, production of the new frequency components in the sound field characteristics, etc. In such situation, precise modelling of both sound generation by a larger blood vessel and transmission of sound through the body tissue for diagnostic purposes is difficult, and only the first approximate steps in adequate describing these processes can be made. An attempt to do this was undertaken in this study. The results obtained here are summarized below.

1. An acoustic model of a larger human blood vessel has been developed. This model takes into account the random statistical nature of the noise sources, the main features of the human chest structure, and permits estimation of some effects connected with the presence a stenotic narrowing in the vessel.

2. On the basis of this model, a relationship (20) has been obtained. It relates the mean statistical characteristic of the noise field to the vessel diameter and mean flow velocity. This relationship also reflects the influence of the geometrical and physical parameters of the human thorax on the propagation of sound waves from the vessel to body surface.

3. The model gives the possibility of illustrating the main features of the mechanism of noise production by a vessel constriction. These are the increase of the noise intensity and generation of the new frequency components in the power spectrum. The components are determined by the mean flow velocity in and the diameter of a constriction.

ACKNOWLEDGEMENTS

The author gratefully acknowledge the financial support of the Alexander von Humboldt Foundation (Germany) and useful comments given by Prof. V. Grinchenko and Prof. P. Költzsch in discussing this work.

1. *Giddens D. P., Mabon R. F., Cassanova R. A.* Measurements of disordered flow distal to subtotal vascular stenosis in the thoracic aorta of canines // Circ. Res.– 1976.– **39**.– P. 112–119.
2. *Tobin R. J., Chang I. D.* Wall pressure spectra scaling downstream of stenoses in steady tube flow // J. Biomech.– 1976.– **9**.– P. 633–640.
3. *Clark C.* Turbulent velocity measurements in a model of aortic stenosis // J. Biomech.– 1976.– **9**.– P. 677–687.
4. *Clark C.* Turbulent wall pressure measurements in a model of aortic stenosis // J. Biomech.– 1977.– **10**.– P. 461–472.
5. *Khalifa A. M., Giddens D. P.* Analysis of disorder in pulsatile flows with application to poststenotic blood velocity measurement in dogs // J. Biomech.– 1978.– **11**.– P. 129–141.
6. *Gosling R. G., King D. H.* Continuous wave ultrasound as an alternative and complement to X-rays in vascular examinations // Reneman,R.S. (ed.), Cardiovascular Applications of Ultrasound.– New York: Elsevier, 1974.– P. 266–282.
7. *Fitzgerald D. E., Carr J.* Doppler ultrasound diagnosis and classification as an alternative to arteriography // Angiology.– (.– 1.– P. 9.75)**26**283–288
8. *Lees R. S., Dewey C. F., Jr.* Phonoangiography: a new noninvasive diagnostic method for studying arterial disease // Proc. Nat. Acad. Sci.– 1970.– **67**.– P. 935–942.

9. *Fredberg J. J.* Pseudo-sound generation at atherosclerotic constrictions in arteries // Bull. Math. Biol.– 1974.– **36**.– P. 143–155.
10. *Fredberg J. J.* Origin and character of vascular murmurs: model studies // J. Acoust. Soc. Amer.– 1977.– **61**.– P. 1077–1085.
11. *Duncan, G. W., Gruber J. O., Dewey C. F, Jr., Myers G. S., Lees, R. S.* Evaluation of carotid stenosis by phonoangiography // New Eng. J. Med.– 1975.– **293**.– P. 1124–1128.
12. *Pitts W. H., III and Dewey C. F., Jr.* Spectral and temporal characteristics of post-stenotic turbulent wall pressure fluctuations // ASME J. Biomech. Eng.– 1979.– **101**.– P. 89–95.
13. *Gavriely N., Palti Y., Alroy G.* Spectral characteristics of normal breath sounds // J. Appl. Physiol.– 1981.– **50**.– P. 307–314.
14. *Kraman S. S.* Determination of the site of production of respiratory sounds by subtraction phonopneumography // Am. Rev. Resp. Dis.– 1980.– **122**.– P. 303.
15. *Charbonneu G., Raccineux J. L., Subraud M., Tuchais E.* An accurate recording system and its use in breath sounds spectral analysis // J. Appl. Physiol.– 1983.– **55**.– P. 1120–1127.
16. *Cohen A., Landsberg D.* Analysis and automatic classification of breath sounds // IEEE Trans. Biomed. Eng.– 1984.– **BME-31**.– P. 585–590.
17. *Vovk I. V., Grinchenko V. T., Krasnyi L. G. and Makarenkov A. P.* Breath sounds: recording and classification problems // Acoust. Phys.– 1994.– **40**.– P. 43–48.
18. *Makarenkov A. P., Rudnitskii A. G.* Diagnosis of lung pathologies by two-channel processing of breathing sounds // Acoust. Phys.– 1995.– **41**.– P. 234–238.
19. *Borisyuk A. O.* Noise generation by flow in pipes in presence of wall obstructions // Rep. Nat. Acad. Sci. Ukr.– 1996.– **11**.– P. 66–70 (in Ukrainian).
20. *Borisyuk A. A.* Noise generated by steady flow in human blood vessels in presence of stenoses // Bionika.– 1998.– **27–28**.– P. 144–151 (in Russian).
21. *Kim B., Corcoran W. K.* Experimental measurement of turbulence spectra distal to stenosis // J. Biomech.– 1974.– **7**.– P. 335–342.
22. *Wang J., Tie B., Welkowitz W., Semmlow J. L., Kostis J. B.* Modeling sound generation in stenosed coronary arteries // IEEE Trans. Biomed. Eng.– **37**.– 1990.– P. 1087–1094.
23. *Wodicka G. R., Stevens K. N., Golub H. L., Cravalho E.G., Shanon D. C.* A model of acoustic transmission in the respiratory system // IEEE Trans. Biomed. Eng.– 1989.– **36**.– P. 925–933.
24. *Wodicka G. R., Stevens K. N., Golub H. L., Shannon D. C.* Spectral characteristics of sound transmission in the human respiratory system // IEEE Trans. Biomed. Eng.– 1990.– **37**.– P. 1130–1134.
25. *Vovk I. V., Zalutskii K. E., Krasnyi L. G.* Acoustic model of the human respiratory system // Akust. Phys..– 1994.– **40**.– P. 676–680.
26. *Corcos G. M.* The resolution of pressure in turbulence // J. Acoust. Soc. Amer.– 1963.– **35**.– P. 192–199.
27. *Borisyuk A. O., Grinchenko V. T.* Vibration and noise generation by elastic elements excited by a turbulent flow // J. Sound Vib.– 1997.– **204**.– P. 213–237.
28. *Martin N. C., Leehey P.* Low wavenumber wall pressure measurements using a rectangular membrane as a spatial filter // J. Sound Vib.– 1977.– **52**.– P. 95–120.
29. *Young D. F.* Fluid mechanics of arterial stenoses // J. Biomech. Eng.– 1979.– **101**.– P. 157–175.
30. *Mirolyubov S. G.* Hydrodynamics of stenosis // Modern Probl. Biomech.– 1983.– N 1.– P. 73–136 (in Russian).
31. *Blake W. K. (ed.)* Mechanics of Flow-Induced Sound and Vibration. In 2 vol..– New York: Academic Press, 1986.– 954 p.
32. *Chase D. M.* Modeling the wavevector-frequency spectrum of turbulent boundary layer wall pressure // J. Sound Vib.– 1980.– **70**.– P. 29–67.
33. *Ffowcs Williams J. E.* Boundary-layer pressures and the Corcos model: a development to incorporate low-wavenumber constraints // J. Fluid Mech.– 1982.– **125**.– P. 9–25.
34. *Smol'yakov A. V., Tkachenko V. M.* Model of a field of pseudosonic turbulent wall pressures and experimental data // Sov. Phys. Akust..– 1991.– **37**.– P. 627–631.
35. *Hwang Y. F., Geib F. E.* Estimation of wavevector-frequency spectrum of turbulent boundary layer wall pressure by multiple linear regression // Proc. International Symposium on Turbulence-Induced Vibrations and Noise of Structures.– 1983, Nov. 13–18, Boston.– P. 13–30.
36. *Fredberg J. J., Holford S. K.* Discrete lung sounds: Crackles (rales) as stress-relaxation quadrupoles // J. Acoust. Soc. Amer.– 1983.– **73**.– P. 1036–1046.

APPENDIX: NOMENCLATURE

H – height of thorax and length of blood vessel;

R – radius of thorax;

a_0 – radius of intact blood vessel;

A – minimum cross-sectional area of blood vessel;

A_0 – unobstructed lumen area of blood vessel;

γ^2 – ratio of the minimum cross-sectional area to the unobstructed lumen area of vessel;

S – severity of stenosis;

ρ – mass density of normal blood;

ρ_0 – mass density of the body tissue;

ν – kinematic viscosity of normal blood;

c – sound speed in normal blood;

c_0 – sound speed in the body tissue;

U – mean flow velocity in the intact vessel;

U_c – convective velocity in the intact vessel;

u – mean flow velocity in the stenosed vessel;

v_* – friction velocity;

Re_{a_0} – Reynolds number of mean flow in the intact vessel;

$Re_{\gamma a_0}$ – Reynolds number of a flow in the stenosed vessel;

Re_{cr} – critical Reynolds number;

r, z – radial and axial coordinates, respectively;

t – time;

ω – circular frequency;

$f = \omega/2\pi$ – frequency;

k – wavenumber in the flow direction;

$k_0 = \omega/c_0$ – acoustic wavenumber of sound waves in the body tissue;

$k_0^{(b)} = \omega/c$ – acoustic wavenumber of sound waves in blood;

$\beta_n^{(1)}$, $\beta_n^{(2)}$ – axial wavenumbers;

$\alpha_n^{(1)}$, $\alpha_n^{(2)}$ – radial wavenumbers;

w_r – radial acceleration in sound wave;

p_t – turbulent wall pressure;

p_0 – acoustic pressure;

$\Psi_n^{(1)}(z)$, $\Psi_n^{(2)}(z)$ – acoustic modes of the thorax volume;

$\omega_n^{(1)}$, $\omega_n^{(2)}$ – cut-off frequencies;

$|S_n^{(1)}(k)|^2$, $|S_n^{(2)}(k)|^2$ – shape functions;

$\Phi_{p_n}^{(1)}(\omega)$, $\Phi_{p_n}^{(2)}(\omega)$ – modal excitation terms;

$\Phi_p(k,\omega)$ – wavenumber-frequency spectrum of turbulent wall pressure;

$P(\omega)$ – power (frequency) spectrum of turbulent wall pressure;

$P_w(r,z,\omega)$ – spectral density of radial acceleration in the measurement point (r,z).